Int. J. Devl Neuroscience 56 (2017) 10–17

Contents lists available at ScienceDirect

International Journal of Developmental Neuroscience

journal homepage: www.elsevier.com/locate/ijdevneu

Nociceptor-like rat dorsal root ganglion neurons express the angiotensin-II AT2 receptor throughout development

Sergio Benitez, Alicia Seltzer, Cristian Acosta*

Instituto de Histología y Embriología de Mendoza (IHEM), Facultad de Ciencias Medicas, Universidad Nacional de Cuyo, 5500, Mendoza, Argentina

ARTICLE INFO

Article history:
Received 17 October 2016
Received in revised form 31 October 2016
Accepted 1 November 2016
Available online 4 November 2016

Keywords:
Angiotensin-II
Sensory neurons
Pain
Ret
IB4
TrkA

ABSTRACT

AT2 receptor (AT2R) plays a functional role in foetal development. Its expression declines in most tissues soon after birth but stays high in sensory areas of the adult nervous system. In the dorsal root ganglia (DRG) the expression pattern of AT2R during development and the identity of the subpopulation expressing it remain unknown. Using a combination of semi-quantitative PCR, western blotting and immunohistochemistry we examined the expression of AT2R at mRNA and protein levels in rat DRGs from embryonic day 15 (E15) until postnatal day 30 (PN30). We found that both AT2R mRNA and protein levels exhibited only minor (statistically non-significant) fluctuations from E15 to PN30. Detailed quantitative analysis of ABC/DAB AT2R staining showed a) that the receptor was present in most neurons at E15 and E18 and b) that postnatally it was predominantly expressed by small DRG neurons. Given that small neurons are putative C-nociceptors and the proposed role of AT2R in neuropathic pain, we next examined whether these AT2R-positive neurons co-localized with Ret and trkA embryonically and with IB4-binding postnatally. Most AT2R-positive neurons expressed trkA embryonically and bound IB4 postnatally. We found strong positive statistically highly significant correlations between AT2R cytoplasmic%intensities and trkA at E15/E18 and with Ret only at E18. Cytoplasmic AT2R also strongly and positively correlated with IB4-binding at PN3, 15 and 30. Our demonstration that a subpopulation of C-nociceptor-like neurons expresses AT2R during development supports a role for this receptor in neuropathic pain.

1. Introduction

Angiotensin-II (Ang-II) receptors are present in the spinal cord and dorsal root ganglia (DRG) (Ahmad et al., 2003; Oldfield et al., 1994). Adult rat and human DRG neurons also express angiotensinogen, the synthesizing enzymes cathepsin-D, ACE and the angiotensin receptors type-1 (AT1R) and type-2 (AT2R) (Anand et al., 2013; Chakrabarty et al., 2008; Patil et al., 2010; Pavel et al., 2008). Thus, a functional renin-angiotensin system is present in DRG neurons and may be involved in the genesis and maintenance of pain (Bali et al., 2014; Chakrabarty et al., 2013; Patil et al., 2010).

Recently, several synthetic drugs with antagonist effect on AT2R were reported to attenuate prostate cancer induced bone pain (Muralidharan et al., 2014), alleviate neuropathic pain (Anand et al., 2015; Rice et al., 2014; Smith et al., 2013) and reverse hypoesthesia induced by *M. ulcerans* in the Buruli ulcer (Anand et al., 2016; Marion et al., 2014). However, the molecular and cellular bases of these actions of AT2R remain poorly understood. To advance our knowledge of the role of AT2R in pathological pain, it is essential to establish what DRG neuronal subpopulations express this receptor.

The DRG comprise subpopulations of neurons with distinct anatomical, electrophysiological and neurochemical characteristics (Krames, 2014; Lawson, 2002; Liu and Ma, 2011). There is a significant correlation between action potential conduction velocity (CV) and cross-sectional area. Thus we recognise three main neuronal subpopulations: neurons with C-fibres (small, slowly conducting, unmyelinated), Aδ (medium, fast conducting, weakly myelinated) and Aα β (large, fastest, heavily myelinated) (Lawson and Waddell, 1991; Lawson, 2002). To play a role in pain, AT2R must be located in nociceptors. This subpopulation includes neurons that bind either the Isolectin-B4 (IB4-positive) or that express trkA (the high-affinity receptor for NGF) or both. Each group contributes ~30% of the C-nociceptors in lumbar DRGs. IB4-positive neurons have C-fibres, are non-peptidergic and predominantly innervate cutaneous and visceral targets (Fang et al., 2006; Zylka et al., 2005). In the adult rat, trkA-positive neurons are peptidergic and variable

Abbreviations: DRG, dorsal root ganglia; GAPDH, glyceraldehyde-3-phosphate dehydrogenase; AT2R, angiotensin-II type 2 receptor; IB4, isolectin B4; Ret, receptor for the glial-derived growth factor; GDNF, glial-derived neurotrophic factor; trkA, tropomyosin receptor kinase A; Adr, Adrenal cortex.

* Corresponding author.
E-mail address: cacosta@fcm.uncu.edu.ar (C. Acosta).

http://dx.doi.org/10.1016/j.ijdevneu.2016.11.001
0736-5748/

in size; include C, Aδ and Aβ nociceptors and mediate the pro-algesic actions of NGF in inflammatory and neuropathic pain (Fang et al., 2005a; Jankowski and Koerber, 2010; Woolf and Ma, 2007).

Developmentally, C-fibres are generated during a second and third wave of embryonic neurogenesis in the DRG and all initially express trkA (Liu and Ma, 2011). In mice, at embryonic day 15.5 some of these trkA-positive neurons began to switch to small Ret-positive. After birth, these neurons also express the GDNF-family of receptors (GFRα1, 2 and 3) and bind IB4 (Golden et al., 2010; Molliver et al., 1997). Where AT2R fits in this complex picture of nociceptor differentiation is unknown.

The purpose of this work was two-fold: first, to describe the pattern of expression of the AT2R mRNA and its protein in the rat DRG throughout development. Second, we aimed to identify what neuronal subpopulation express AT2R, using classification by size and also the phenotypic markers Ret/trkA and IB4-binding.

2. Materials and methods

We used Wistar rats of 2 embryonic (E15 and E18) and 3 post-natal (PN3, 15 and 30) ages. E0 was defined as the day of mating; PN0 was the day of birth. All procedures had been approved by the Institutional Animal Care and Use Committee (CICUAL #31/2014) of the School of Medical Sciences, UNCuyo.

2.1. Semi-quantitative RT-PCR

mRNA levels were determined by RT-PCR following previously published protocols (Kunda et al., 2014; Marsh et al., 2012). mRNA was extracted using RNeasy (Qiagen) from whole L4/L5 DRGs (this equates to 4 DRG per animal) at each age (5 rats per age). cDNA was synthesized from 200 ng total RNA using the M-MLV kit (Promega). AT2R and GAPDH mRNA were detected using Taq polymerase (Invitrogen) with 35 and 30 cycles, respectively. We performed a negative control containing RNA instead of cDNA to rule out genomic DNA contamination.

Primers sequences were: AT2R forward 5′-CAACTTCAGTTTTGCTGCCAC-3′; reverse 5′-CAGGTCCAAAGAGCCAGTCAT-3′, predicted size 335 bp. For GAPDH, forward 5′-GGTGCTGAGTATGTCGTGGA-3′ and reverse 5′-GGATGCAGGGATGATGTTCT-3′, predicted size 340 bp. All primers were custom-designed and checked using Primer-BLAST. Images of the RT-PCR SYBR Safe (Molecular Probes) stained agarose gels were acquired with an LAS-4000 system (Fujifilm) and quantified with ImageJ software, see Kunda et al. (2014).

2.2. Western blots (WB)

WB were performed as previously described (Acosta et al., 2014). Total protein was extracted from whole L4/L5 DRGs at each age (3 rats per age) using Laemmli buffer supplemented with a protease/phosphatase inhibitor cocktail (HALT, Thermofisher). Samples of ∼20 μg of total protein were run in 8–10% polyacrylamide gels and transferred to a PVDF membrane (Amersham) before blotting. Membranes were probed with 1:1000 goat anti-AT2R (Santa Cruz Biotechnology Cat# sc-48452, K15, RRID:AB_2225720) and 1:2000 mouse anti-α-tubulin (eBioscience, 14–4502-80, RRID:AB_1210457) as loading control. The anti-AT2R antibody has been characterized and it is selective unlike other commercially available antibodies (Anand et al., 2013; Hafko et al., 2013).

Protein bands were developed using ECLPlus (Amersham) and visualized with LAS-4000 system (Fujifilm). WBs were replicated 3 times and quantification was conducted as previously described (Kunda et al., 2014).

2.3. Immunohistochemistry

L4/L5 DRGs from 4 rats per age were fixed in Zamboni's fixative and stored overnight at 4 °C in 30% sucrose. Tissue was then frozen at −80 °C and cut in serial transverse 7 μm cryostat sections.

a. ***Avidin-biotin complex (ABC) immunohistochemistry*** was performed as previously described (Acosta et al., 2012, 2014). The anti-AT2R was used at 1:200. For comparisons between different ages, all sections were incubated simultaneously and treated identically at all stages.
b. ***Double immunofluorescence*** was conducted following previously published protocols (Acosta et al., 2014). Tissue was incubated sequentially in the first primary antibody overnight at 4 °C and in secondary antibody appropriate for that primary antibody for 1hr at room temperature. We used goat anti-AT2R 1:200 (see Section 2.2); rabbit anti-Ret 1:500 (Santa Cruz Biotechnology, sc-167, RRID:AB_631317) and mouse anti-trkA 1:500 (AbD Serotec, 7045-7040, RRID:AB_620277). Secondary antibodies: anti-goat Alexa-594, anti-mouse Alexa-488 and anti-rabbit Alexa-488, all 1:400 (Molecular Probes, Invitrogen). For IB4-binding, tissue was incubated with IB4 conjugated with Alexa-488 (1:500) (Bergman et al., 1999).

2.4. Image analysis

All analysis was performed as previously detailed, see (Fang et al., 2006), on images captured on a Nikon 80i microscope and the measures were performed using HCImage (Hamamatsu). In the co-localization studies, only neurons with visible nuclei were measured. An average of 6–8 fields at ×40 from mid-sections of L4/L5 DRGs were all captured at the same time with identical settings. The cross sectional area and mean cytoplasmic pixel density were determined for each neuron. The mean pixel densities of the 5 most intensely stained and the 5 least intensely stained neurons in the analysed section provided 100% and 0% values respectively.

Neurons were classed by size. For embryonic and early post-natal DRG neurons only 2 groups can be discerned: small and large. At E15, small, mechanical-insensitive neurons are those with areas ≤100 μm^2 while at E18 the limit is ∼120 μm^2 (Lawson and Biscoe, 1979; Lechner et al., 2009). Based on expression of the neurofilament of 200 kDa, which labels large, myelinated neurons (Lawson et al., 1984), the boundary moves to ∼300 μm^2 at PN3 and ∼350 μm^2 at PN15 (Beland and Fitzgerald, 2001). At PN30 we classed them as small (≤400 μm^2, mostly C-fiber neurons), medium-sized (400–800 μm^2, mostly Aδ-neurons) and large (>800 μm^2 mostly Aα β neurons) see (Fang et al., 2005b).

2.4.1. Neurons classed as positive

For each antibody/marker, neurons were classed as positive on the basis of percentage values of neurons that were blindly classed subjectively as clearly stained above background. A subjective score of 1 (visible staining) corresponded to objective AT2R values of ≥20% which were therefore classed as clearly positive.

2.5. Statistics

Because our data failed the DíAgostino-Pearson test for normality, non-parametric tests were used. Results are shown as means ± SEM and comparison between multiple treatment groups was with one way Kruskal-Wallis ANOVA with Dunn's multiple comparisons test. Comparison between 2 treatments was with Mann-Whitney test. All tests were performed with Prism 5 (GraphPad). A level of $p < 0.05$ was considered statistically significant. Correlations were tested with Spearman's non-parametric test.

Significance is indicated on all graphs by $^{*}p < 0.05$, $^{**}p \leq 0.01$, $^{***}p \leq 0.001$, $^{****}p \leq 0.0001$.

3. Results

3.1. Dorsal root ganglia express AT2R throughout development

Using real-time semi-quantitative PCR we found that AT2R mRNA was already detectable at embryonic day 15 (E15) and was present in all ages we examined up to postnatal day 30 (PN30) (Fig. 1A). Adrenal cortex (Adr) was used as positive control. Quantification of the mRNA levels of AT2R relative to GAPDH showed no significant differences amongst any age examined (mean ± SEM ratios ranging from 0.60 ± 0.10 at E15 to 0.67 ± 0.08 at PN30, n = 5, P = 0.9321, Fig. 1B).

Albeit AT2R mRNA levels were similar throughout development, post-transcriptional regulation could result in uneven protein expression of this receptor. Thus, we next used WB analysis to address this possibility. Despite small inter-animal variation (especially noticeable at E16) there were no apparent differences in the expression level of AT2R between the different ages (Fig. 1C). This was confirmed by quantification, with mean ± SEM ratios of AT2R to α-tubulin ranging from 0.27 ± 0.09 at E16 to 0.51 ± 0.05 at E18, n = 3, P = 0.2511, Fig. 1D). Thus, AT2R expression in the DRG is detectable and remains essentially unaltered from E15 to PN30.

We must consider that DRGs contain non-neuronal cells such as vascular endothelium which can express AT2R. However, AT2R mRNA and protein are probably predominantly neuronal because in rats, neurons plus fibres are a large proportion of DRG volume. Also, there is scant evidence for AT2R expression in fibroblasts and glial cells, the other cell types present in the DRG. Nevertheless, we went on to assess a) whether AT2R was indeed expressed by DRG neurons and b) by what neuronal subpopulation, as this has important bearings on the possible involvement of AT2R in pathological pain.

3.2. A subpopulation of small-sized neurons in the DRG expresses AT2R

Fig. 2A shows representative photomicrographs of AT2R ABC immunostaining in normal L4/L5 mid DRG sections of different ages. The bottom plot shows the mean cytoplasmic%intensities (±SEM) for E15 (43.5 ± 1.8, n = 158), E18 (39.6 ± 2.0, n = 129), PN3 (45.6 ± 1.9, n = 146), PN15 (59.3 ± 2.7, n = 128) and PN30 (54.0 ± 2.8, n = 119). AT2R mean%intensities were significantly higher at PN15 and PN30 than at E15 and E18, with AT2R levels at PN15 also higher than at PN3 (P < 0.001).

Image analysis showed that AT2R cytoplasmic%intensities was significantly and positively correlated with cell area for E15 (Spearmanís correlation $r_s = +0.36$, P < 0.001) and E18 ($r_s = +0.23$, P < 0.001) (Fig. 2B). However, this pattern was reverted and the AT2R cytoplasmic%intensities were significantly and negatively correlated with cell area at PN3, 15 and 30 (r_s values of −0.22, −0.44 and −0.39 respectively, P < 0.001). Notice that DRG neurons with cytoplasmic%intensities (i.e. relative percentages of maximum) of AT2R ≥20% were classed as AT2R-positive, and those with <20% as AT2R-negative (grey band, see Section 2.4).

To elucidate what neuronal subpopulation preferentially expresses AT2R, we classed the neurons according to their cross-sectional areas (Fig. 2C). At E15, AT2R levels were higher in larger neurons with no significant differences at E18 or PN3. At all other ages examined, AT2R cytoplasmic%intensities were significantly higher in small than in medium/large neurons (P < 0.0001, Fig. 2C).

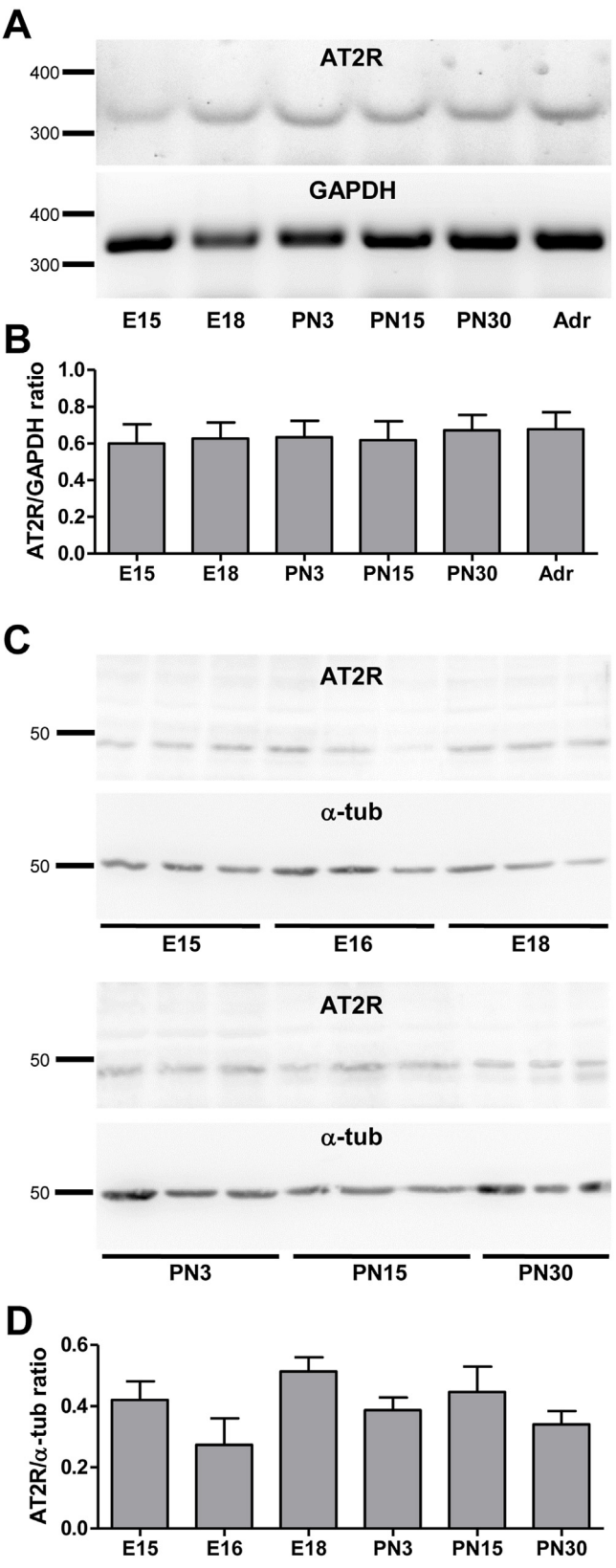

Fig. 1. Representative gels (A) and corresponding bar graphs (B) of semi quantitative RT-PCR amplification products for AT2R mRNA relative to GAPDH. Note that the ratio of AT2R/GAPDH is similar at all ages examined (indicated at the bottom of the gels). mRNA was extracted from 5 different animals for each age. Adrenal cortex (Adr) mRNA was used as a positive control. In all experiments, amplification of GAPDH was run in parallel to normalize samples. Data presented as the mean ± SEM of the calculated ratios. C. Representative Western blots showing the expression of AT2R from L4/5 DRG at different ages (each lane corresponds to a different rat). Mouse α-tubulin was used as loading control. D. Quantification of the WBs showed that L4/5 DRGs expressed comparatively similar levels of AT2R at all ages examined.

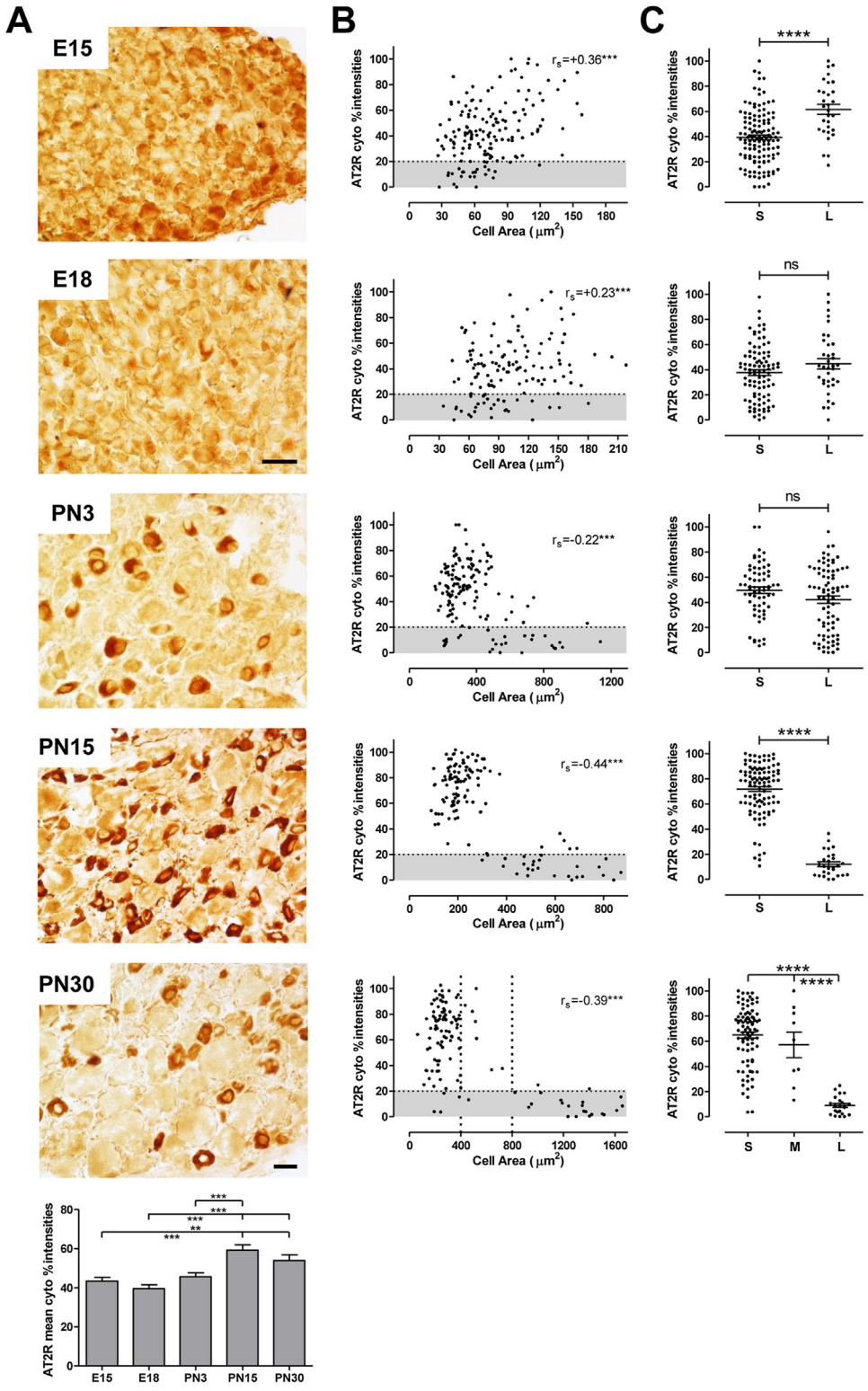

Fig. 2. A. Representative photomicrographs of ABC/DAB staining of AT2R in L5 DRG mid-sections at the indicated ages and quantification of mean AT2R cytoplasmic%intensities. Scale bars are 20 µm. B. Plots of AT2R cytoplasmic%intensities versus cross-sectional areas (in μm^2) at each age examined. Spearmanís correlation values (r_s) are indicated in each plot. The grey band indicates negative levels. AT2R expression switched from predominant in large neurons at E15/18 to small neurons postnatally. C. Scatter plots comparing AT2R levels in small (S) versus large (L) neurons for E15, E18, PN3 and PN15. At PN30, DRG neurons are classed as S, medium (M) and L. Significance is indicated by $^{**}p \leq 0.01$, $^{***}p \leq 0.001$, $^{****}p \leq 0.0001$.

3.3. *Embryonic AT2R: from trkA to ret*

Prenatally, DRG neurons switch from NGF-dependence for survival and differentiation to depend on other neurotrophins, most notably from the GDNF-derived family of trophic factors (Liu and Ma, 2011; Molliver et al., 1997). This means switching from trkA-positive at E15 to Ret-positive later on (Golden et al., 2010; Kashiba et al., 2001). This switch is particularly important as a large

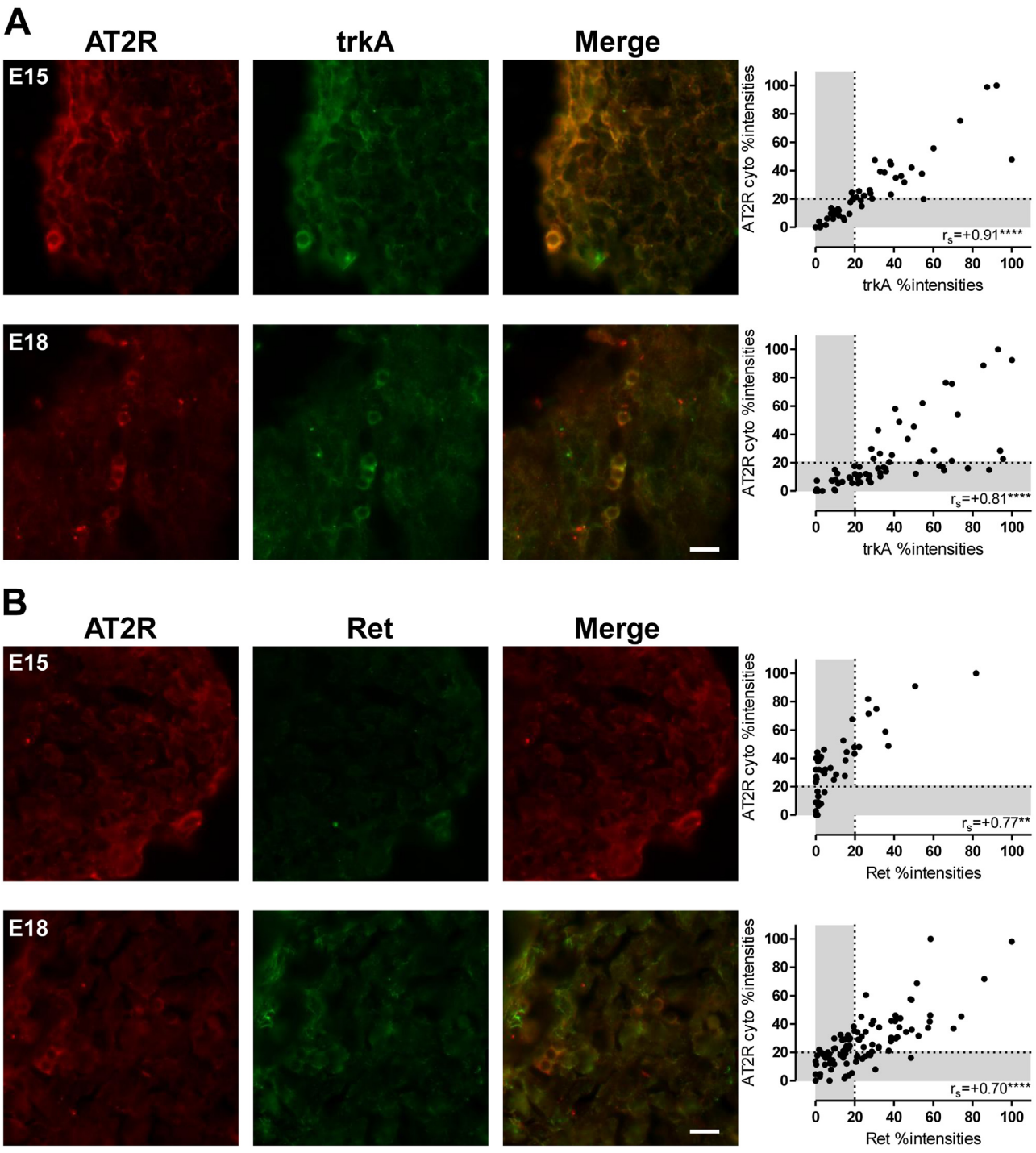

Fig. 3. Representative 100× photomicrographs of AT2R (red), trkA (green) and AT2R/trkA overlap (yellow) (A) or AT2R (red) with Ret (green) and AT2R/Ret overlap (yellow) (B) in L5 DRG at E15 and E18. The far right plots in A show significant positive Spearmanís correlations for AT2R and trkA at both ages. In B, there is significant positive Spearmanís correlations for AT2R and Ret at E15 and E18, but most AT2R-positive neurons are Ret negative at E15. Grey bands indicate negative levels. Scale bar is 10 μm. Significance is indicated by $^{**}p \leq 0.01$, $^{****}p \leq 0.0001$. (For interpretation of the references to colour in this figure legend, the reader is referred to the web version of this article.)

number of these Ret-positive neurons will become IB4-binding (IB4-positive) nociceptors postnatally. Thus, we examined the co-localization of AT2R with trkA (Fig. 3A) and Ret (Fig. 3B) at E15 and E18. As expected, at E15 and E18 AT2R cytoplasmic%intensities were highly positively correlated with trkA. Notice that at E18 some trkA-positive neurons did not express AT2R.

At E15, most DRG neurons were Ret-negative and most AT2R-positive cells were not co-localized with it. This pattern changes at E18 with at least some AT2R-positive neurons co-localizing with Ret. This expression profile suggests a possible developmental switch in the subpopulation expressing AT2R.

3.4. IB4-binding DRG neurons express AT2R after birth

Considering that a) postnatally most AT2R-positive DRG neurons were small and b) that AT2R probably plays a role in

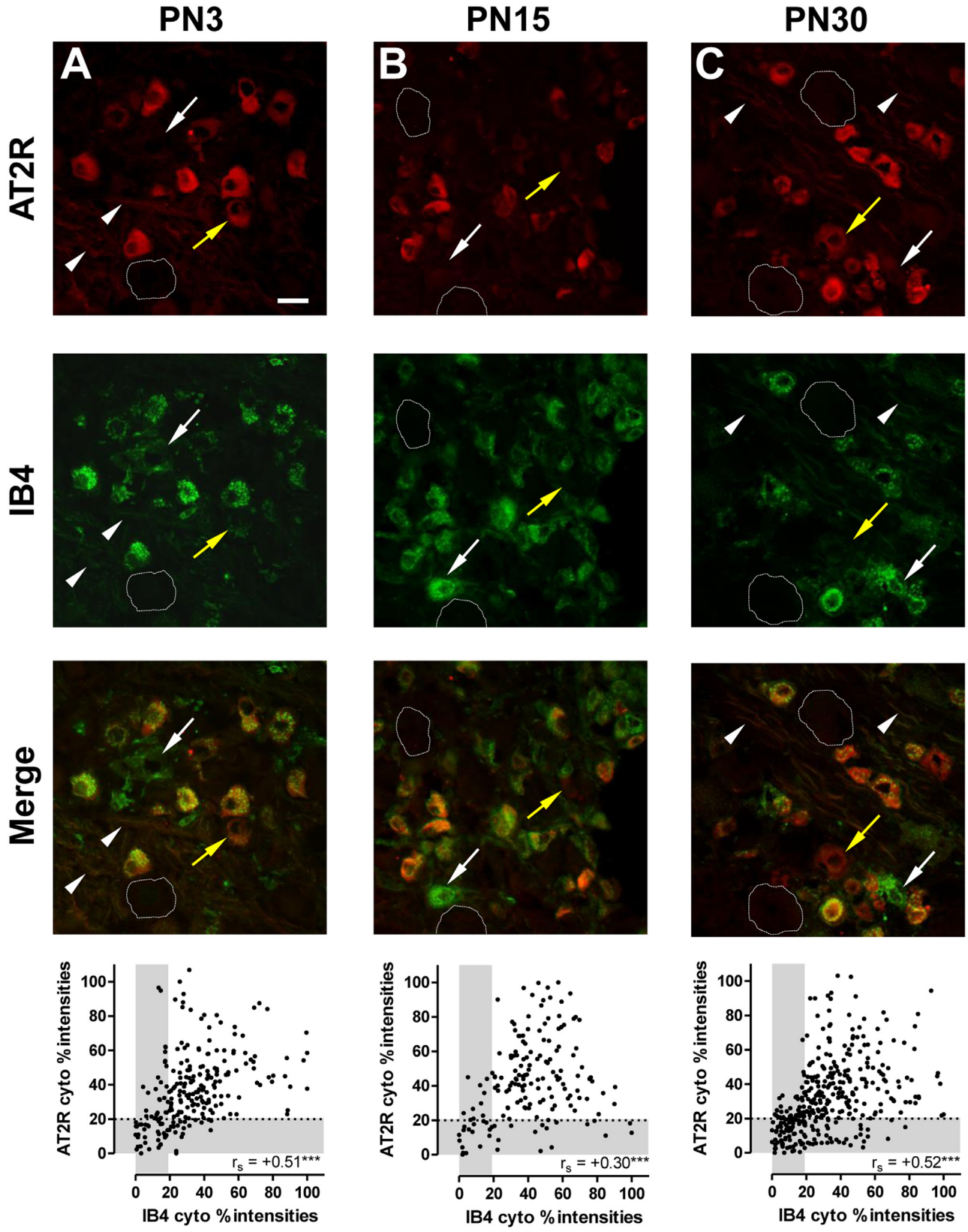

Fig. 4. Most AT2R-positive neurons (red) bind IB4 (green) at PN3 (A), PN15 (B) and PN30 (**C**). Scale bar represents 25 μm. Neurons negative for AT2R and IB4 are delineated by a dotted-line. White arrows point out AT2R-negative/IB4-positive neurons while yellow arrows point at AT2R-positive/IB4-negative neurons. Arrowheads show thinly-unmyelinated IB4-binding fibres also stained for AT2R. Image analysis shows strong positive Spearmanís correlations between AT2R cytoplasmic%intensities and cytoplasmic IB4 staining. Significance is indicated by $^{***}p \leq 0.001$. (For interpretation of the references to colour in this figure legend, the reader is referred to the web version of this article.)

nociception, we examined whether its expression was restricted to the IB4-positive subpopulation. We found that cytoplasmic%intensities of AT2R and IB4 were strongly positively correlated at PN3 ($r_s = +0.51$, $P < 0.001$, Fig. 4A), PN15 ($r_s = +0.30$, $P < 0.001$, Fig. 4B) and PN30 ($r_s = +0.52$, $P < 0.001$, Fig. 4C). The proportion of AT2R-positive neurons that were IB4-positive was significant and similar at the three ages examined: 74% (125 out of 168) at PN3; 81% (112 out of 138) at PN15 and 84% (201 out of 242) at PN30. Notice that AT2R staining is clearly visible on unmyelinated IB4-stained thin fibres (arrowheads in Fig. 4A,C).

4. Discussion

This study demonstrates that AT2R expression levels in DRG neurons remain constant from early foetal life until adulthood. Interestingly, at E15 most trkA-positive neurons express AT2R while at PN3 (and onwards) the receptor is predominantly expressed by IB4-binding C-nociceptors.

4.1. AT2R in the whole DRG

This study is the first demonstration that AT2R mRNA and protein levels in the DRG remain essentially unchanged from E15 until PN30. Our finding agrees with the pattern of expression described for the main sensory areas of the CNS. AT2R is detected early (E13) in development and its expression increased and further stabilized in these areas during perinatal and adult life (Nuyt et al., 1999). In human embryos at stages 14–16 AT2R mRNA detected by *in situ* hybridization appeared in tissues that contain derivatives of neural crest cells (Schutz et al., 1996). Taken together, the evidence suggests that AT2R plays a role in central and peripheral nervous system maturation and early functioning. Notice that in other systems AT2R expression changes significantly from foetal to adult life. For example, it goes up in the brainstem of adult rat and mouse (Gao et al., 2012; Yu et al., 2010).

Ang-II has been proposed as a growth factor during organogenesis (Tebbs et al., 1999) and it exhibits neuritogenic activity acting through AT2R in DRG neurons (Anand et al., 2013; Chakrabarty et al., 2008). Despite these recent advances, the precise function of Ang-II/AT2R during the development of the DRG remains unknown.

4.2. Small DRG neurons express AT2R

At embryonic and early postnatal life, rat DRG neurons can only be classed as small and large (Beland and Fitzgerald, 2001; Lawson and Biscoe, 1979). Large A-fiber RT97-positive neurons are born from E12 to E15, peaking at E13, whereas the future IB4-binding small C-fiber non-peptidergic neurons are born later at E13–16, peaking at E14 (Kitao et al., 1996). Thus at E15 we already have got two neuronal populations: one destined to be A-fibres mechanoreceptors and other IB4-positive nociceptors. Our data suggests that at this age both populations express AT2R but at later stages is down-regulated in the A-fibres while remains strongly expressed in small putative C-nociceptors. The predominant expression of AT2R in small neurons postnatally agrees with the initial report by Chakrabarty et al. of expression in small and medium diameter DRG neurons (Chakrabarty et al., 2008). Our finding is also in agreement with a study of human DRG cells in culture, where AT2R-positive neurons were detected in a population of small diameter (Anand et al., 2013).

4.3. IB4-binding C-nociceptors express AT2R postnatally

Most trkA-positive neurons express AT2R at E15 while at E18 there are two subpopulations expressing it: one that is trkA-positive and other that is Ret-positive. Postnatally (from PN3 onwards) AT2R is mostly present in IB4-positive neurons. Given that adult IB4-positive neurons start off as trkA-positive at E15 and then become small Ret-positive, it seems that AT2R expression accompanies the development of the C-nociceptors.

Because most IB4-positive DRG small neurons are C-fiber nociceptors in rat (Fang et al., 2006) and we show that ~80% of AT2R-positive neurons are small and IB4-positive, we conclude that the majority of AT2R-positive neurons are non-peptidergic C-fiber nociceptors. Several studies have shown that small non-IB4-positive neurons are often trkA-positive (Fang et al., 2005a, 2006; Molliver et al., 1995). Thus, the remaining 20% AT2R-positive neurons are probably trkA-positive but this remains to be determined.

It has been speculated that because Ang-II often co-localize with Substance P and CGRP in trkA-positive DRG neurons, this neuropeptide may modulate nociception via an autocrine mechanism (Patil et al., 2010). Instead, our finding that AT2R is in IB4-positive non-peptidergic C-nociceptors implies that Ang-II acts via a paracrine mechanism.

The temporal changes in AT2R localization are probably associated with a wider role in neuronal differentiation during embryonic life, while playing a more restricted role in nociception after birth and into adulthood.

Taken together, our results provide novel evidence for an involvement of AT2R a) during the differentiation of and b) in pain mediated by IB4-binding C-nociceptors.

Funding

This work was supported by the Agencia Nacional para la Promoción de la Ciencia y la Tecnología (Argentina) [grant number PICT-2014-0651] to C.A. and by a postdoctoral fellowship granted to S.B. by CONICET (Argentina)

Acknowledgements

We would like to thank Prof. Mabel Foscolo for her technical assistance and Prof. Sally Lawson for useful comments on the size distributions of DRG neurons throughout development.

References

Acosta, C., McMullan, S., Djouhri, L., Gao, L., Watkins, R., Berry, C., Dempsey, K., Lawson, S.N., 2012. HCN1 and HCN2 in Rat DRG neurons: levels in nociceptors and non-nociceptors, NT3-dependence and influence of CFA-induced skin inflammation on HCN2 and NT3 expression. PLoS One 7, e50442.

Acosta, C., Djouhri, L., Watkins, R., Berry, C., Bromage, K., Lawson, S.N., 2014. TREK2 expressed selectively in IB4-binding C-fiber nociceptors hyperpolarizes their membrane potentials and limits spontaneous pain. J. Neurosci. 34, 1494–1509.

Ahmad, Z., Milligan, C.J., Paton, J.F., Deuchars, J., 2003. Angiotensin type 1 receptor immunoreactivity in the thoracic spinal cord. Brain Res. 985, 21–31.

Anand, U., Facer, P., Yiangou, Y., Sinisi, M., Fox, M., McCarthy, T., Bountra, C., Korchev, Y.E., Anand, P., 2013. Angiotensin II type 2 receptor (AT2 R) localization and antagonist-mediated inhibition of capsaicin responses and neurite outgrowth in human and rat sensory neurons. Eur. J. Pain 17, 1012–1026.

Anand, U., Yiangou, Y., Sinisi, M., Fox, M., MacQuillan, A., Quick, T., Korchev, Y.E., Bountra, C., McCarthy, T., Anand, P., 2015. Mechanisms underlying clinical efficacy of angiotensin II type 2 receptor (AT2R) antagonist EMA401 in neuropathic pain: clinical tissue and in vitro studies. Mol. Pain 11, 38.

Anand, U., Sinisi, M., Fox, M., MacQuillan, A., Quick, T., Korchev, Y., Bountra, C., McCarthy, T., Anand, P., 2016. Mycolactone-mediated neurite degeneration and functional effects in cultured human and rat DRG neurons: mechanisms underlying hypoalgesia in *Buruli ulcer*. Mol. Pain 12.

Bali, A., Singh, N., Jaggi, A.S., 2014. Renin-angiotensin system in pain: existing in a double life? J. Renin Angiotensin Aldosterone Syst. 15, 329–340.

Beland, B., Fitzgerald, M., 2001. Influence of peripheral inflammation on the postnatal maturation of primary sensory neuron phenotype in rats. J. Pain 2, 36–45.

Bergman, E., Carlsson, K., Liljeborg, A., Manders, E., Hokfelt, T., Ulfhake, B., 1999. Neuropeptides, nitric oxide synthase and GAP-43 in B4-binding and RT97 immunoreactive primary sensory neurons: normal distribution pattern and changes after peripheral nerve transection and aging. Brain Res. 832, 63–83.

Chakrabarty, A., Blacklock, A., Svojanovsky, S., Smith, P.G., 2008. Estrogen elicits dorsal root ganglion axon sprouting via a renin-angiotensin system. Endocrinology 149, 3452–3460.
Chakrabarty, A., Liao, Z., Smith, P.G., 2013. Angiotensin II receptor type 2 activation is required for cutaneous sensory hyperinnervation and hypersensitivity in a rat hind paw model of inflammatory pain. J. Pain 14, 1053–1065.
Fang, X., Djouhri, L., McMullan, S., Berry, C., Okuse, K., Waxman, S.G., Lawson, S.N., 2005a. TrkA is expressed in nociceptive neurons and influences electrophysiological properties via Nav1.8 expression in rapidly conducting nociceptors. J. Neurosci. 25, 4868–4878.
Fang, X., McMullan, S., Lawson, S.N., Djouhri, L., 2005b. Electrophysiological differences between nociceptive and non-nociceptive dorsal root ganglion neurones in the rat in vivo. J. Physiol. 565, 927–943.
Fang, X., Djouhri, L., McMullan, S., Berry, C., Waxman, S.G., Okuse, K., Lawson, S.N., 2006. Intense isolectin-B4 binding in rat dorsal root ganglion neurons distinguishes C-fiber nociceptors with broad action potentials and high Nav1.9 expression. J. Neurosci. 26, 7281–7292.
Gao, J., Chao, J., Parbhu, K.J., Yu, L., Xiao, L., Gao, F., Gao, L., 2012. Ontogeny of angiotensin type 2 and type 1 receptor expression in mice. J. Renin Angiotensin Aldosterone Syst. 13, 341–352.
Golden, J.P., Hoshi, M., Nassar, M.A., Enomoto, H., Wood, J.N., Milbrandt, J., Gereau, R.W., Johnson Jr., E.M., Jain, S., 2010. RET signaling is required for survival and normal function of nonpeptidergic nociceptors. J. Neurosci. 30, 3983–3994.
Hafko, R., Villapol, S., Nostramo, R., Symes, A., Sabban, E.L., Inagami, T., Saavedra, J.M., 2013. Commercially available angiotensin II At(2) receptor antibodies are nonspecific. PLoS One 8, e69234.
Jankowski, M.P., Koerber, H.R., (2010) Neurotrophic Factors and Nociceptor Sensitization.
Kashiba, H., Uchida, Y., Senba, E., 2001. Difference in binding by isolectin B4 to trkA and c-ret mRNA-expressing neurons in rat sensory ganglia. Brain Res. Mol. Brain Res. 95, 18–26.
Kitao, Y., Robertson, B., Kudo, M., Grant, G., 1996. Neurogenesis of subpopulations of rat lumbar dorsal root ganglion neurons including neurons projecting to the dorsal column nuclei. J. Comp. Neurol. 371, 249–257.
Krames, E.S., 2014. The role of the dorsal root ganglion in the development of neuropathic pain. Pain Med. 15, 1669–1685.
Kunda, P.E., Cavicchia, J.C., Acosta, C.G., 2014. Lipopolysaccharides and trophic factors regulate the LPS receptor complex in nodose and trigeminal neurons. Neuroscience 280, 60–72.
Lawson, S.N., Biscoe, T.J., 1979. Development of mouse dorsal root ganglia: an autoradiographic and quantitative study. J. Neurocytol. 8, 265–274.
Lawson, S.N., Waddell, P.J., 1991. Soma neurofilament immunoreactivity is related to cell size and fibre conduction velocity in rat primary sensory neurons. J. Physiol. 435, 41–63.
Lawson, S.N., Harper, A.A., Harper, E.I., Garson, J.A., Anderton, B.H., 1984. A monoclonal antibody against neurofilament protein specifically labels a subpopulation of rat sensory neurones. J. Comp. Neurol. 228, 263–272.
Lawson, S.N., 2002. Phenotype and function of somatic primary afferent nociceptive neurones with C-, Adelta- or Aalpha/beta-fibres. Exp. Physiol. 87, 239–244.
Lechner, S.G., Frenzel, H., Wang, R., Lewin, G.R., 2009. Developmental waves of mechanosensitivity acquisition in sensory neuron subtypes during embryonic development. EMBO J. 28, 1479–1491.
Liu, Y., Ma, Q., 2011. Generation of somatic sensory neuron diversity and implications on sensory coding. Curr. Opin. Neurobiol. 21, 52–60.
Marion, E., Song, O.R., Christophe, T., Babonneau, J., Fenistein, D., Eyer, J., Letournel, F., Henrion, D., Clere, N., Paille, V., Guerineau, N.C., Saint Andre, J.P., Gersbach, P., Altmann, K.H., Stinear, T.P., Comoglio, Y., Sandoz, G., Preisser, L., Delneste, Y., Yeramian, E., Marsollier, L., Brodin, P., 2014. Mycobacterial toxin induces analgesia in buruli ulcer by targeting the angiotensin pathways. Cell 157, 1565–1576.
Marsh, B., Acosta, C., Djouhri, L., Lawson, S.N., 2012. Leak K(+) channel mRNAs in dorsal root ganglia: relation to inflammation and spontaneous pain behaviour. Mol. Cell. Neurosci. 49, 375–386.
Molliver, D.C., Radeke, M.J., Feinstein, S.C., Snider, W.D., 1995. Presence or absence of TrkA protein distinguishes subsets of small sensory neurons with unique cytochemical characteristics and dorsal horn projections. J. Comp. Neurol. 361, 404–416.
Molliver, D.C., Wright, D.E., Leitner, M.L., Parsadanian, A.S., Doster, K., Wen, D., Yan, Q., Snider, W.D., 1997. IB4-binding DRG neurons switch from NGF to GDNF dependence in early postnatal life. Neuron 19, 849–861.
Muralidharan, A., Wyse, B.D., Smith, M.T., 2014. Analgesic efficacy and mode of action of a selective small molecule angiotensin II type 2 receptor antagonist in a rat model of prostate cancer-induced bone pain. Pain Med. 15, 93–110.
Nuyt, A.M., Lenkei, Z., Palkovits, M., Corvol, P., Llorens-Cortes, C., 1999. Ontogeny of angiotensin II type 2 receptor mRNA expression in fetal and neonatal rat brain. J. Comp. Neurol. 407, 193–206.
Oldfield, B.J., Allen, A.M., Hards, D.K., McKinley, M.J., Schlawe, I., Mendelsohn, F.A., 1994. Distribution of angiotensin II receptor binding in the spinal cord of the sheep. Brain Res. 650, 40–48.
Patil, J., Schwab, A., Nussberger, J., Schaffner, T., Saavedra, J.M., Imboden, H., 2010. Intraneuronal angiotensinergic system in rat and human dorsal root ganglia. Regul. Pept. 162, 90–98.
Pavel, J., Tang, H., Brimijoin, S., Moughamian, A., Nishioku, T., Benicky, J., Saavedra, J.M., 2008. Expression and transport of Angiotensin II AT1 receptors in spinal cord, dorsal root ganglia and sciatic nerve of the rat. Brain Res. 1246, 111–122.
Rice, A.S., Dworkin, R.H., McCarthy, T.D., Anand, P., Bountra, C., McCloud, P.I., Hill, J., Cutter, G., Kitson, G., Desem, N., Raff, M., 2014. EMA401, an orally administered highly selective angiotensin II type 2 receptor antagonist, as a novel treatment for postherpetic neuralgia: a randomised, double-blind, placebo-controlled phase 2 clinical trial. Lancet 383, 1637–1647.
Schutz, S., Le Moullec, J.M., Corvol, P., Gasc, J.M., 1996. Early expression of all the components of the renin-angiotensin-system in human development. Am. J. Pathol. 149, 2067–2079.
Smith, M.T., Woodruff, T.M., Wyse, B.D., Muralidharan, A., Walther, T., 2013. A small molecule angiotensin II type 2 receptor (AT(2)R) antagonist produces analgesia in a rat model of neuropathic pain by inhibition of p38 mitogen-activated protein kinase (MAPK) and p44/p42 MAPK activation in the dorsal root ganglia. Pain Med. 14, 1557–1568.
Tebbs, C., Pratten, M.K., Broughton, P.F., 1999. Angiotensin II is a growth factor in the peri-implantation rat embryo. J. Anat. 195 (Pt. 1), 75–86.
Woolf, C.J., Ma, Q., 2007. Nociceptors–noxious stimulus detectors. Neuron 55, 353–364.
Yu, L., Zheng, M., Wang, W., Rozanski, G.J., Zucker, I.H., Gao, L., 2010. Developmental changes in AT1 and AT2 receptor-protein expression in rats. J. Renin Angiotensin Aldosterone Syst. 11, 214–221.
Zylka, M.J., Rice, F.L., Anderson, D.J., 2005. Topographically distinct epidermal nociceptive circuits revealed by axonal tracers targeted to Mrgprd. Neuron 45, 17–25.